

Advanced Energy Management Infrastructure for Electric Vehicles: An Optimized Dual-Input Bidirectional Power Converter Strategy with Integrated Solar Energy Harvesting

Nelipudi Varshini

Dept. of Electrical and Electronics Engineering, Ramireddy Subbarami Reddy Engineering College, Andhra Pradesh, India.

Abstract - This comprehensive study provides a thorough evaluation of an optimized Bidirectional Dual-Input Single-Output (BDISO) DC-DC converter designed specifically for Electric Vehicle (EV) platforms. By merging Photovoltaic (PV) solar technology alongside advanced Maximum Power Point Tracking (MPPT) control, the architecture establishes a highly effective framework for balancing and directing power flow between multiple complementary sources. This dual-input functionality optimizes system-wide energy efficiency while establishing resilient power links within modern electric vehicles. The analysis delivers an in-depth breakdown of operational principles, automotive system integration, technological benefits, and validation methodologies. Practical applications are underscored through real-world operational scenarios, followed by an evaluation of ongoing engineering issues and breakthrough solutions. Simulated under various operational regimes and voltage fluctuations within the MATLAB/Simulink environment, the findings confirm that this bidirectional network dramatically improves EV power sustainability and marks a crucial evolutionary milestone for smart grid-connected transport systems.

Keywords-Bidirectional DC-DC Converters, Dual-Input Single-Output (DISO), Maximum Power Point Tracking (MPPT), Photovoltaic (PV) Infrastructure, Smart Electrical Grid, Energy Management Systems, Electric Vehicle (EV) Integration.

1. INTRODUCTION

The urgent global mandate for ecologically responsible and sustainable transit networks has driven unprecedented acceleration in the mainstream adoption of Electric Vehicles (EVs). As structural paradigms within the automotive sector shift completely toward vehicular electrification, a paramount developmental emphasis has emerged centered on maximizing the thermodynamic efficiency, structural grid reliability, and clean energetic footprint of EV power management systems. A central pillar of this ongoing technological evolution is the direct coordination of renewable energy frameworks—most

notably on-board or station-integrated Photovoltaic (PV) arrays to actively fulfill EV electricity requirements and minimize macro-level greenhouse emissions.

Within this expanding eco-system, the Bidirectional Dual-Input Single-Output (BDISO) DC-DC power converter serves as a vital bridging element for next-generation vehicular powertrains. This converter facilitates seamless, highly responsive bidirectional energy exchanges between the high-voltage automotive battery bank and external grid or local generation infrastructure. The versatile multi-port architecture of the BDISO system makes it perfectly suited for incorporating variable renewable installations like solar arrays directly into standard EV replenishment networks.

Pairing PV solar capture directly with electric mobility delivers several critical performance enhancements. First, it supplies a distributed secondary energy stream that significantly extends driving range, offering major benefits in regions where access to centralized charging hubs remains dispersed or unavailable. Second, the utilization of ambient solar irradiation satisfies critical ecological benchmarks by reducing dependency on fossil-fuel-dominated utility grids. Nonetheless, managing a highly dynamic PV-to-vehicle interface introduces unique technical challenges, particularly regarding high-precision tracking during changing cloud cover and managing complex multi-directional power routings.

To resolve these operational difficulties, this research presents the engineering design, control architecture, and rigorous testing of a specialized BDISO DC-DC converter optimized for next-generation EV environments. The proposed topology embeds dedicated solar inputs governed by state-of-the-art Maximum Power Point Tracking (MPPT) algorithms. The core objective of this study focuses on detailing the structural viability, efficiency profiles, and operational flexibility of the BDISO configuration in maintaining steady energy routing between PV units, utility grids, and vehicular storage. Leveraging the specialized MATLAB/Simulink ecosystem for rigorous dynamic modeling, this work refines multi-port conversion stages and control loops to ensure peak system efficiency and reliable execution,

paving the way toward an environmentally secure and resilient transport sector.

2. CHARGING PARADIGMS AND INFRASTRUCTURE TOPOLOGIES

Modern electric transport networks employ multiple charging pathways and grid communication frameworks. These methodologies vary fundamentally based on current types, infrastructure requirements, and communication complexities.

2.1 Smart Charging Protocols

Description: Smart charging represents an integrated operational model where advanced digital control networks and real-time bidirectional telemetry manage the rate and duration of vehicular replenishment based on macro-grid parameters, current utility pricing signals, and local distribution thresholds. **Benefits:** Mitigates dangerous localized overloading across substation assets, lowers charging costs for end-users via automated off-peak optimization, and increases overall grid operational safety. **Use Case:** Deployed primarily in intelligent smart-home environments, municipal hubs, and commercial vehicle depots tied into time-of-use (ToU) utility tariffs and dynamic demand-response mechanisms.

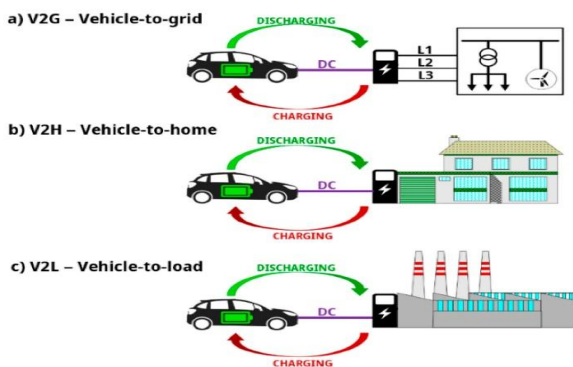


Fig. 1. Smart Charging EV energy management.

2.2 Vehicle-to-Grid (V2G) Systems

Description: Vehicle-to-Grid (V2G) frameworks allow a completely automated, high-frequency bidirectional power exchange between the vehicle's internal high-voltage battery and the public utility system. This interaction effectively treats millions of parked EVs as a giant, highly distributed energy storage system. **Benefits:** Provides critical grid stabilization resources including active frequency regulation, spinning reserves, peak load shaving, and localized financial returns for vehicle owners through energy market participation. **Use Case:** Utilized when vehicles are idle during periods of severe grid stress or extreme power demand, allowing rapid energy extraction to prevent localized blackouts.

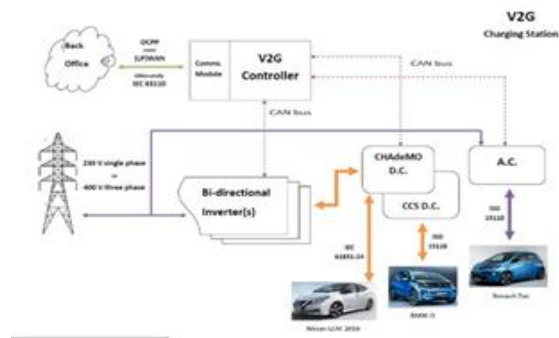


Fig. 2. Vehicle-to-Grid (V2G) architecture for EV energy management.

2.3 Vehicle-to-Building (V2B) Integration

Description: V2B applications route energy stored inside vehicular batteries directly into isolated building distribution boards or microgrids, augmenting localized building power systems during peak consumption hours. **Benefits:** Exponentially increases localized structural power resilience, offers vital emergency backup capacity during utility outages, and smooths building demand spikes to minimize building capacity penalties. **Use Case:** Frequently deployed in industrial complexes, multi-family smart buildings, and isolated residential installations equipped with native energy management platforms.

2.4 Comprehensive Grid Services and Virtual Power Plants (VPPs)

Description: Grid support services coordinate aggregated fleets of connected EVs into single unified networks. By applying predictive machine-learning models, market trading rules, and centralized orchestration, these frameworks actively balance the rapid power fluctuations introduced by volatile renewable generation sources. **Benefits:** Enhances the system-wide security, hosting capacity, and flexibility of the electrical grid while generating diverse revenue flows across participating industrial partners. **Use Case:** Implemented by transmission system operators (TSOs) and energy aggregators utilizing fleets of plugged-in vehicles as a scalable Virtual Power Plant (VPP).

2.5 Conductive Power Transfer

Description: Conductive charging refers to the direct, physical connection of electrical current paths between the supply source and the vehicle via specialized cables, safety-interlocked pins, and heavy-duty plugs. **Types:** Standardized into Level 1 AC residential pathways, Level 2 multi-phase commercial systems, and extreme high-voltage DC Fast Charging stations. **Use Case:** Represents the dominant method for home garaging, commercial parking facilities, and high-throughput highway transit corridors.

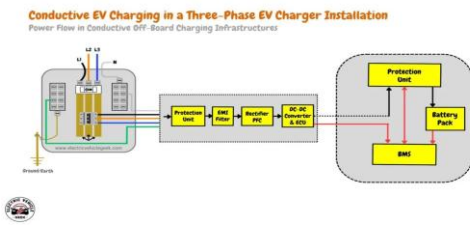


Fig. 3. Conductive charging infrastructure using cable-based EV charging system.

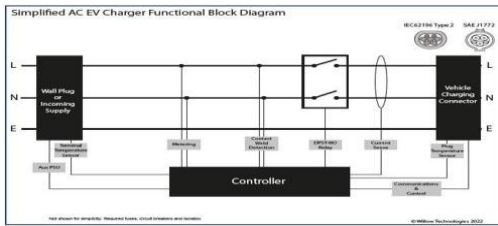


Fig. 4. Simplified AC EV Charger Functional Block Diagram.

3. STANDARDIZATION OF EV CHARGING CLASSES

EV charging levels are structured into distinct regulatory classes characterized by specific voltage levels, current types, and power output ranges. Table 1 outlines these standard parameters, detailing their performance attributes and practical operational profiles.

Table : EV Charging Classes

EV Charging Level	Voltage & Current Configuration	Typical Installation Site	Average Charging Rate	Replenishment Duration
Level 1 (AC)	120 V AC (Single-Phase)	Residential / Domestic Outlets	4 Miles / Hour	30+ Hours (Full Charge)
Level 2 (AC)	240 V AC (Split/Multi-Phase)	Workplaces / Public Stations	12-30 Miles / Hour	8-12 Hours (Overnight)
Level 3 (DC)	480+ V DC (Fast Charging)	Commercial Hubs / Highway Stops	3-15 Miles / Minute	30 Minutes to 80% Capacity



Fig. 5. Classification of EV charging levels and infrastructure.

4. MATHEMATICAL CHARACTERIZATION AND MODELING OF PV ARRAYS

To accurately simulate the dynamic response of solar energy collection stages, the underlying silicon photovoltaic mechanism is modeled based on semiconductor transport equations. A standard solar cell is represented by a light-dependent current source configured in anti-parallel with a non-linear p-n junction diode, accompanied by parasitic series and shunt resistances that reflect real-world material losses.

The internal dark current flowing across the diode interface is governed by the classic Shockley semiconductor expression, detailed in Equation (1):

$$i_d = i_0 * [e^{(q * V_c) / (a * k * T_c)} - 1] \quad (1)$$

Where:

- i_d represents the diode dark current (A)
- i_0 defines the reverse diode saturation current (A)
- V_c represents the terminal voltage across the cell (V)
- q signifies the elementary electron charge constant (1.602×10^{-19} C)
- a denotes the empirical diode ideality factor
- k represents the Boltzmann constant (1.381×10^{-23} J/K)
- T_c defines the absolute cell operational temperature (K)

Accounting for the generated photocurrent, the net terminal output current under ideal conditions equals the difference between the light-induced photocurrent and the dark diode current, as shown in Equation (2):

$$I = I_L - i_d \quad (2)$$

To accurately account for physical power dissipation across non-ideal interfaces, localized ohmic losses are modeled using a lumped-parameter framework. This model introduces a series resistance (R_s) to capture grid-line and contact resistance, along with a parallel shunt resistance (R_{sh}) to represent junction leakage currents. Extrapolating this to a multi-module practical

solar array yields the complete behavioral expression detailed in Equation (3):

$$I = I_L - i_0 * [e^{(V + I * R_s) / (V_t * a)} - 1] - (V + I * R_s) / R_{sh} \quad (3)$$

Equation (3) yields the final terminal current, which varies dynamically under changing environmental inputs, including surface solar irradiance, wind cooling speed, and ambient temperature profiles.

5. STRUCTURAL TOPOLOGY AND CIRCUIT DYNAMICS OF THE DISO CONVERTER

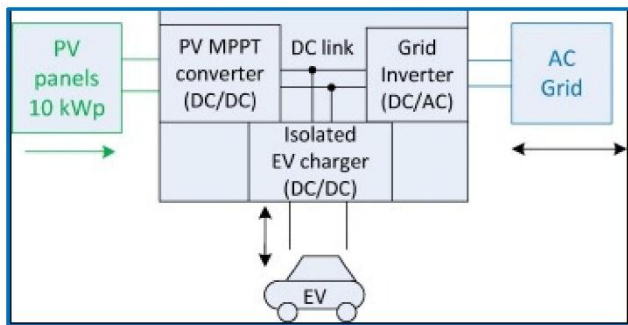


Fig. 6. PV integrated BDISO converter architecture for electric vehicle charging.

The Dual-Input Single-Output (DISO) DC-DC power converter features a highly integrated layout designed to interface simultaneously with distinct power sources. The primary structural assembly consists of an input voltage channel (V_{in}), two independent high-speed MOSFET power switches (S_1, S_2), dual fast-recovery power diodes (D_1, D_2), filtering inductors (L_1, L_2), and smoothing output capacitors (Co_1, Co_2) delivering steady power across independent load segments (Ro_1, Ro_2).

A key advantage of this multi-port conversion stage is its ability to process a single input and generate two separate output voltage levels. This makes the architecture uniquely well-suited for powering various subsystems within electric vehicles. When configured as a boost converter, the primary output voltage (Vo_1) can be significantly stepped up, while the secondary lower-voltage rail (Vo_2) is regulated via buck converter operation. Compared to conventional multi-port configurations, KY converters, or SEPIC networks, this integrated DISO configuration features lower component counts, reduced voltage/current ripple, higher volumetric power density, and superior overall conversion efficiency.

The dynamic operation of the DISO converter is divided into four distinct switching states based on the duty cycles of switches S_1 and S_2 :

- **Mode 1** [$0 < t < t_1$]: Switches S_1 and S_2 are simultaneously closed. Energy stored within inductor L_1 discharges to charge inductor L_2 while actively

supplying power to the buck load Ro_2 . This state terminates precisely at the end of the $(d_1 - d_2/2)T_s$ interval. Zero-voltage switching is achieved on S_1 due to the resonant path established between L_1, L_2 , and Co_2 during the previous state transition, while diodes D_1 and D_2 remain reverse-biased.

- **Mode 2** [$t_1 < t < t_2$]: Switch S_1 is commanded open while S_2 remains closed. The energy stored in inductor L_2 discharges directly into load Ro_2 . Simultaneously, energy is transferred to inductor L_1 . In this state, diode D_2 remains reverse-biased. This operational phase lasts for a duration defined by the d_2T_s interval.

- **Mode 3** [$t_2 < t < t_3$]: The circuit behavior in this mode replicates the conditions of Mode 1, re-establishing parallel energetic tracking paths.

- **Mode 4** [$t_3 < t < t_4$]: Both primary switches S_1 and S_2 are turned off. The stored energy inside inductors L_1 and L_2 discharges completely to sustain the primary loads Ro_1 and Ro_2 through the freewheeling diode loops.

6. OPTIMIZATION VIA PERTURB AND OBSERVE (P&O) MPPT CONTROL

To extract peak power from the PV array under changing environmental conditions, a specialized Perturb and Observe (P&O) tracking algorithm is implemented. The P&O technique is widely favored in commercial applications due to its algorithmic simplicity, low computational overhead, and proven reliability.

The control loop operates by periodically perturbing the array's terminal operating voltage and measuring the resulting change in power output. If the perturbation yields a positive change in power ($\Delta P > 0$), the operating point is moving toward the peak of the P-V curve, and the controller continues perturbing the voltage in the same direction. Conversely, if the power delta becomes negative ($\Delta P < 0$), the system has passed the maximum power point, prompting the algorithm to reverse the perturbation direction. This iterative tracking loop continuously adjusts the converter's duty cycle, ensuring the solar array operates at its peak efficiency under all conditions.

7. SIMULATION ARCHITECTURE AND DYNAMIC PERFORMANCE VALIDATION

To validate the performance of the proposed converter layout and tracking algorithms, a series of detailed multi-domain models were developed inside the MATLAB/Simulink environment. The simulation testing framework includes full representations of a grid-tied solar array, bidirectional battery management loops, three-phase inversion bridges, harmonic output filters, and the multi-port DISO converter system.

The system was evaluated across multiple test scenarios to verify its dynamic response and stability:

• Operational Case 1 (Solar-to-Battery Dominion):

The solar array is simulated under steady peak irradiance. The MPPT controller quickly locks onto the peak power point, providing steady current to charge the vehicle's high-voltage battery. The battery's State of Charge (SoC) shows a steady, linear increase, confirming stable energy transfer and minimal ripple in the converter stages.

• Operational Case 2 (Grid-Assisted Replenishment):

This scenario simulates zero or reduced solar generation (e.g., heavy cloud cover or night conditions). The grid-side inverter activates smoothly, drawing power from the utility grid to maintain a steady charging rate for the vehicle's battery. Current waveforms remain clean, showing that the filtering networks effectively suppress switching harmonics.

• Operational Case 3 (Vehicle-to-Grid Feedback Mode):

This test verifies the bidirectional capability of the system. Power flows in reverse from the vehicle's battery back into the local distribution grid, simulating peak-shaving operations. The converter maintains stable voltage regulation during this reverse power flow, demonstrating its ability to support grid stability during peak demand periods.

8. CONCLUSION

This study has presented a detailed design and performance evaluation of an optimized Bidirectional Dual-Input Single-Output (BDISO) DC-DC power converter tailored for electric vehicles. By incorporating integrated solar harvesting capabilities and an efficient P&O MPPT tracking algorithm, the proposed architecture provides a flexible framework for managing multi-directional power flow. The simulation results confirm the system's high efficiency and stability across various operating modes, including solar charging, grid-connected operation, and V2G energy feedback. Ultimately, this multi-port conversion layout offers a reliable and scalable solution for next-generation EV power architectures, supporting the broader integration of electric transport with smart grid networks.

9. REFERENCES

- [1] M. Yaich, M. R. Hachicha and M. Ghariani, "Modeling and simulation of electric and hybrid vehicles for recreational vehicle," 2015 16th International Conference on Sciences and Techniques of Automatic Control and Computer Engineering (STA), 2015, pp. 181-187, doi: 10.1109/STA.2015.7505098.
- [2] H. Xiaotao et al., "Operation and Maintenance System of Electric Vehicles' Charging and Discharging Facilities Based on Repository," 2021 IEEE 3rd International Conference on Civil Aviation Safety and Information Technology (ICCASIT), 2021, pp.

894-897, doi: 10.1109/ICCASIT53235.2021.9633471.

- [3] P. Kumar, S. A. Deokar and A. M. Kate, "Design and Implementation of Ecofriendly vehicle and its Impact on Environment," 2018 3rd International Conference on Communication and Electronics Systems (ICCES), 2018, pp. 224-228, doi: 10.1109/CESYS.2018.8724014.
- [4] M. M. Hasan, M. El Baghdadi and O. Hegazy, "Energy Management Strategy in Electric Buses for Public Transport using ECOdriving," 2020 Fifteenth International Conference on Ecological Vehicles and Renewable Energies (EVER), 2020, pp. 1-8, doi: 10.1109/EVER48776.2020.9243130.
- [5] R. Betala and H. Kumar Naidu, "A Review to Innovative a Green Electric Vehicle for Future," 2022 10th International Conference on Emerging Trends in Engineering and Technology - Signal and Information Processing (ICETET-SIP-22), 2022, pp. 01-06, doi: 10.1109/ICETET-SIP-2254415.2022.9791571.
- [6] P. Aji, D. A. Renata, A. Larasati and Riza, "Development of Electric Vehicle Charging Station Management System in Urban Areas," 2020 International Conference on Technology and Policy in Energy and Electric Power (ICT-PEP), 2020, pp. 199-203, doi: 10.1109/ICTPEP50916.2020.9249838.
- [7] J. Tao, D. Huang, D. Li, X. Yang and C. Ling, "Pricing strategy and charging management for PV-assisted electric vehicle charging station," 2018 13th IEEE Conference on Industrial Electronics and Applications (ICIEA), 2018, pp. 577-581, doi: 10.1109/ICIEA.2018.8397782.
- [8] M. Anwar et al., "State of Charge Monitoring System of Electric Vehicle Using Fuzzy Logic," 2018 International Conference on Sustainable Energy Engineering and Application (ICSEEA), 2018, pp. 34-38, doi: 10.1109/ICSEEA.2018.8627131.
- [9] T. Li et al., "An Optimal Design and Analysis of a Hybrid Power Charging Station for Electric Vehicles Considering Uncertainties," IECON 2018 - 44th Annual Conference of the IEEE Industrial Electronics Society, 2018, pp. 5147-5152, doi: 10.1109/IECON.2018.8592855.